Abdominal Aortic Aneurysm: From Clinical Imaging to Realistic Replicas

Sergio Ruiz de Galarreta
Mechanical Department,
Tecnun,
Universidad de Navarra,
San Sebastián 20018, Spain

Aitor Cazón[1]
CEIT and Mechanical Department,
Tecnun,
Universidad de Navarra,
San Sebastián 20018, Spain
e-mail: acazon@tecnun.es

Raúl Antón
Mechanical Department,
Tecnun,
Universidad de Navarra,
San Sebastián 20018, Spain

Ender A. Finol
Department of Biomedical Engineering,
The University of Texas at San Antonio,
San Antonio, TX 78249

The goal of this work is to develop a framework for manufacturing nonuniform wall thickness replicas of abdominal aortic aneurysms (AAAs). The methodology was based on the use of computed tomography (CT) images for virtual modeling, additive manufacturing for the initial physical replica, and a vacuum casting process and range of polyurethane resins for the final rubberlike phantom. The average wall thickness of the resulting AAA phantom was compared with the average thickness of the corresponding patient-specific virtual model, obtaining an average dimensional mismatch of 180 μm (11.14%). The material characterization of the artery was determined from uniaxial tensile tests as various combinations of polyurethane resins were chosen due to their similarity with ex vivo AAA mechanical behavior in the physiological stress configuration. The proposed methodology yields AAA phantoms with nonuniform wall thickness using a fast and low-cost process. These replicas may be used in benchtop experiments to validate deformations obtained with numerical simulations using finite element analysis, or to validate optical methods developed to image ex vivo arterial deformations during pressure-inflation testing. [DOI: 10.1115/1.4025883]

Keywords: AAA replica, additive manufacturing, vacuum casting, tensile strength

Introduction

An abdominal aortic aneurysm (AAA) is a permanent focal dilatation of the abdominal aorta in the infrarenal segment to 1.5 times its normal diameter [1], causing 1.3% of all deaths among men aged 65–85 in developed countries. The ability to predict the rupture of the abdominal aorta is a concern for both vascular surgeons and patients, since it is based on statistical in vivo data [2] and numerical patient-specific analysis. An AAA rupture is associated with the diameter of the aneurysm, but the use of finite element analysis has indicated that an AAA rupture is also highly related to peak wall stress [3–6]. Patient-specific aneurysm phantoms have been created in fabrication laboratories to replicate the response of the abdominal aorta. These replicas are built by combining medical images and conventional manufacturing techniques such as additive manufacturing (AM) and injection molding [7–9]. To achieve reliable outcomes from both numerical and in vitro experiments, materials whose mechanical properties have a stress-strain curve similar to those of the aneurysm wall should be used to build the replicas [10]. These curves change spatially along the aorta and are dependent on the patient's age, gender, and the ratio of elastin and collagen; the aneurysmal aorta is stiffer compared to the healthy aorta [11].

The primary objective of this work is to develop and apply a new modeling and manufacturing process for patient-specific artery replicas with nonuniform wall thickness, with a focus on developing physiologically realistic AAA phantoms. This is the first time, to the authors' knowledge, that a methodology is reported for manufacturing arteries with nonuniform wall thickness distributions. Artery replicas were manufactured by using computed tomography (CT) images to generate virtual models, AM to make the initial physical model, and vacuum casting in combination with commercially available polyurethane resins (PURs) and casting wax, to build the final phantom. The material characterization was assessed from uniaxial tensile experiments. These replicas can be useful to validate deformations obtained with numerical simulations with the small deformations that occur in a phantom placed in a benchtop apparatus subject to pulsatile flow and pressure. To this end, the compliance of the patient-specific replicas will be accurate at small strain ranges and they will have individual geometric characteristics, including regional variations of wall thickness.

Methods

The vacuum casting technique was chosen as the preferred manufacturing method to build an arterial replica. The process involves pouring liquid polyurethane resins (PURs) under vacuum into a silicon mold that contains a hollow cavity with the desired shape. The mold was previously obtained by taking as a reference a master model printed with an AM technology. The steps for creating the artery replica are illustrated in Fig. 1.

Virtual Abdominal Aorta. The patient-specific AAA geometry was obtained following the acquisition of the subject's contrast-enhanced CT images from Allegheny General Hospital (Pittsburgh, PA) following an Institutional Review Board approved protocol. The medical images were segmented using in-house image segmentation software (AAAVASC, University of Texas at San Antonio, San Antonio, TX), which is capable of identifying the boundaries of the lumen inner and outer wall surfaces [12]. The segmentation algorithms have been extensively validated [12,13] and used to quantify the geometry of patient-specific AAA models [14,15], identify classifiers of ruptured/

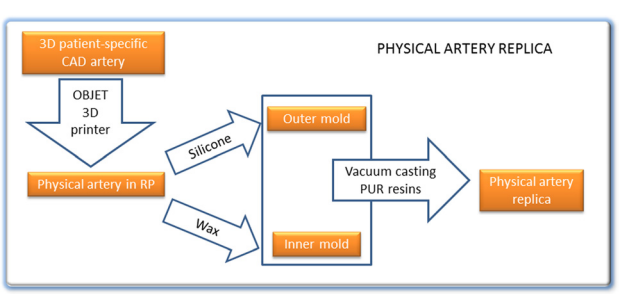

Fig. 1 Flow chart describing the artery replication process

[1]Corresponding author.

Contributed by the Bioengineering Division of ASME for publication in the JOURNAL OF BIOMECHANICAL ENGINEERING. Manuscript received July 12, 2013; final manuscript received October 29, 2013; accepted manuscript posted October 31, 2013; published online December 4, 2013. Assoc. Editor: Jonathan Vande Geest.

Fig. 2 Partition lines for the artery, with their proper connector pins (left), AM artery within the mold and filling the frame with silicon (center), and the final outer mold once cut open (right)

unruptured AAA populations based on surface curvature estimation [16], and quantify the effect of patient-specific wall thickness in the ensuing wall biomechanics [17]. In the context of this work, the AAA segmentation involves the AAA sac as along with the common iliac arteries.

The CT-based reconstruction was converted to a stereolithography format (*.STL). The AAA geometry was subsequently manipulated using MAGICS v16.02 (Materialise, Leuven, Belgium) to prepare a virtual model for the AM. With MAGICS, the artery was cut along several partition lines, while assuring the correct positioning of each part relative to the other parts with the use of connector pins, in order to facilitate the vacuum casting process (see Fig. 2).

Physical Artery Replica. The physical replica was created following the methodology depicted. We used the AM printer OBJET EDEN 330 (Stratasys Ltd., Minneapolis, MN, USA), which is based on the PolyJet technology featuring print resolutions of 42, 84, and 16 μm in the X, Y, and Z-axes, respectively. The printing material for the artery was the general purpose Fullcure 720. Once printed, the outer and the inner molds were built by using the AM artery as the master model.

For the outer mold (see Fig. 2), the printed artery with its proximal and distal boundary openings blocked with Plasticine® was rigidly fit inside a methacrylate frame. A viscous mix of silicone and a catalyst (SLM VTX 950, SLM Solutions GmbH, Lübeck, Germany) at a 10:1 ratio was poured inside the frame until it was completely filled and the artery entirely covered. The frame was then placed inside an oven at 45 °C to cure for 24 h. Once cured, the mold was cut open and the artery was removed, leaving the mold cavity, which accurately replicated the outer surface of the artery. Two ports were made in the mold to enable the subsequent steps of wax and resin injections: one in the proximal region for the wax injection and another close to the artery's maximum diameter for the resin injection. The inner mold (see Fig. 3) was made of WA-70 wax (SLM) with a melting point between 68 °C and 70 °C. To build this wax mold, the AM artery was placed into the silicone mold and both were preheated at 40 °C for 24 h. The wax was in a liquid state after being melted in an oven at 70 °C and it was poured through the silicon mold's upper port. Once poured, the silicone mold containing the additive manufactured artery and the liquid wax inside it were placed inside the oven at 40 °C to slowly solidify the wax. Once in a solid state, the silicone mold was opened and the wax was removed from the interior of

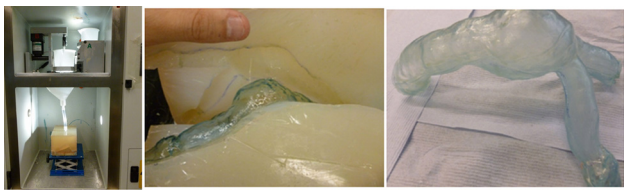

Fig. 4 Vacuum casting process for the artery: silicon mold with the wax mold inside ready for casting the PUR resin (left), opening the mold to remove the artery (center), and the final artery replica (right)

the AM artery. With the outer and inner molds created, we followed a casting process using am MCP 4/01 vacuum casting machine (SLM Solutions GmbH, Lübeck, Germany). The raw material used to replicate the artery was the commercial resin SLM PUR (a transparent rubber with high resistance to UV light).

The first step of the casting process was to place the silicone (outer) mold with the wax (inner) mold together with the two components (A and B) of the PUR in the vacuum chamber (see Fig. 4). The resin was degassed, mixed, and poured into the mold. When the mold was filled, the vacuum was released and the mold was placed in an oven at 45 °C to cure the resin. After 24 h of curing, the oven temperature was increased to 85 °C to melt the inner wax. At the end of the melting process (approximately 3 h), the silicone mold was opened and the rubberlike artery removed. The entire process, as illustrated in Fig. 1, can be completed in less than 4 days. The approximate cost of fabricating an artery replica (i.e., the AAA phantom) with this protocol, not including the cost of machine-hours and man-hours, is 135 €(∼176 USD): 80 €(∼104 USD) for the 3D printing, 40 €(∼52 USD) for the silicone material, and 15 €(∼20 USD) for the PUR resins. The phantom was inspected to quantify its geometric accuracy; 30 randomly distributed rectangular samples were cut from the artery replica with a scalpel and, from each sample, ten thicknesses were randomly measured by using a digital caliper with a resolution of 10 μm. Simultaneously, twelve thicknesses from each of the corresponding samples of the virtual aorta model were computationally measured. These measurements were statistically analyzed by calculating the mean and standard deviation for each sample and a comparison was made between the real and virtual aorta model. The mean and standard deviations for each physical and virtual sample were calculated using the ten real and twelve virtual measurements, respectively.

Physical Artery Properties. With the manufacturing protocol defined, the next step was to measure the mechanical properties of the phantom material candidates to yield stress-strain curves that can be compared to the known healthy and aneurysmal abdominal aorta properties [11]. To this end, various rubberlike materials were created using the commercially available SLM bicomponent PUR SLM 7140, 7160, and 7190 (A and B) as the base material. The A and B components were mixed in various ratios to obtain a range of diverse resins. In addition, another sample of the specimen was printed with the 3D printer using the

Fig. 3 Process for the inner mold: silicone mold with the AM artery (left), filling the mold with liquid wax (center), and opening the AM artery to remove the wax mold (right)

rubberlike material Fullcure 980 Tango Black Plus. With this range of materials, several tensile specimens were created and tested to obtain stress-strain curves that are as physiologically realistic as possible. The tensile test specimens were designed in accordance with ASTM D412 Type B. All specimens were preconditioned at 20 °C (±1 °C) and 40% (±5%) relative humidity prior to testing. The tensile tests were performed on the specimens to generate force-extension data using an INSTRON MINI 44 (Instrom Worldwide, Norwood, MA) tensile test machine. Each sample was subjected to a cross-head speed of 3.4 mm/min until failure with preconditioning of 10 cycles to 7.5% of the gauge length to avoid the Mullins effect [18]. The load-displacement outputs from the tensile test machine were normalized to the stress-strain data. The strain was defined as

$$\varepsilon = \frac{\Delta l}{l_0}$$

where Δl is the change in the length of the specimen at any time and l_0 is its original length. The true stress (Cauchy) was used, assuming that the testing materials were incompressible and that the volume did not change during the tests

$$\sigma = \frac{F}{A^*}$$

$$A^* = \frac{A_0 l_0}{l_0 + \Delta l}$$

where F is the force required and A^* is the area at any instant.

Results

Wall Thickness. The average and standard deviations of the wall thicknesses are shown in Table 1. The percentage differences refer to the difference between the wall thickness of the physical replica (phantom) and the virtual model. It was found that the physical artery had thicker walls with the average difference for all the samples at 11.14%, which is equivalent to an absolute difference of 180 μm.

Stress-Strain Curves. Large human arteries, as most soft tissues, exhibit a nonlinear mechanical behavior characterized by a stress-strain curve with convexity toward the horizontal axis; small increases in stress result in large stretches (toe region) and are followed by a quasi-linear behavior (at moderate strains). The polyurethane resins tested in this research exhibited almost linear stress-strain curves, which is a behavior that is similar to most man-made materials. While it was not possible to replicate the entire hyperelastic soft tissue behavior, we obtained a reasonably analogous behavior of the resins in the toe region of both the normal and the aneurysmal abdominal aorta [11]. The stress strain curves resulting from the uniaxial tensile testing are shown in Fig. 5. The response of a typical healthy abdominal aorta and an AAA [18] obtained by Raghavan et al. [11] under zero-stress conditions and at room temperature are superimposed in this chart for comparison purposes. With the available resins and the proper mixing ratio, it was possible to achieve a good correlation with the population-averaged healthy aorta and AAA tissues. In the case of the healthy aortic tissue, the toe region (0–0.2 strain) is approximated with the M7140 resin (RA100 RB38) with a RMS error for the stress and the stiffness (the slope of the stress-strain curves: $E = \sigma/\varepsilon$) of 42.86 kPa and 0.66 MPa respectively, based on 200 data points. Similarly, the response of the AAA tissue was also reasonably approximated with the M7160 resin (RA100 RB69), but only up to a 0.15 strain. The RMS error for the stress of this correlation was 42.75 kPa, while the RMS error for the stiffness was 1.28 MPa based on 150 data points.

However, it is noteworthy that the Raghavan et al. curves were obtained under a zero-stress condition, while in vivo tissue is exposed to a stressed configuration. Other researchers [19–22] have analyzed the stressed configuration of large and small vessels, obtaining mean peak stresses between 130 kPa and 180 kPa depending on the artery. If we consider 150 kPa as the mean value of the state of stress in vivo, the present methodology is still suitable since the AAA tissue can be represented by the linear region of the stress-strain curve and a good approximation would be obtained for any patient-specific artery by modifying the PUR mixing ratio. For the individual AAA used in this work, the most appropriate PUR mixing ratio would be the 7190 (RA100RB75) resin, which better approximates the AA and AAA tissue with an RMS error for stiffnesses of 1.79 MPa and 1.45 MPa, respectively and an RMS error for stresses of 275.12 kPa and 108.23 kPa, respectively. These errors were the lowest ones for the tested PUR resins for both the stress and stiffness RMS and for both the AA and AAA arteries. Considering that the range of stiffnesses for each point varies from 2.18 MPa to 7.39 MPa in these points, the RMS error is acceptable. Nevertheless, it must be stated that only a few mixtures have been tested and any alternative outcome can be achieved testing different mixing ratios of the PUR resins. In summary, although the stress-strain dependency is not linear in an in vivo loading condition, for small strain a linear stress-strain relationship is a reasonably good approximation. This methodology allows us to match that linearity with a synthetic material.

Table 1 Thicknesses of the physical and virtual arteries

	Artery replica				
	Virtual		Real		
Sample	Average (mm)	Standard (mm)	Average (mm)	Standard (mm)	Difference (%)
1	1.842	0.45	1.956	0.23	6.18
2	1.724	0.26	1.912	0.23	10.90
3	1.617	0.12	1.948	0.19	20.50
4	1.577	0.08	1.899	0.22	20.40
5	1.628	0.09	2.017	0.24	23.90
6	1.712	0.27	1.948	0.35	13.80
7	1.531	0.04	1.546	0.32	1.01
8	1.561	0.07	1.571	0.22	0.65
9	1.546	0.08	1.644	0.25	6.36
10	1.591	0.09	1.645	0.28	3.42
11	1.752	0.21	1.750	0.28	−0.09
12	1.658	0.18	1.699	0.31	2.47
13	1.624	0.14	1.648	0.25	1.51
14	1.583	0.1	1.618	0.21	2.22
15	1.530	0.05	1.641	0.4	7.27
16	1.565	0.061	1.685	0.37	7.67
17	1.644	0.136	1.797	0.36	9.31
18	1.893	0.384	1.914	0.26	1.14
19	1.949	0.529	2.038	0.29	4.57
20	1.703	0.213	2.209	0.35	29.68
21	1.575	0.079	2.299	0.21	45.93
22	1.602	0.102	2.113	0.16	31.95
23	1.599	0.117	2.127	0.28	33.03
24	1.964	0.579	2.296	0.37	16.88
25	1.550	0.056	1.550	0.4	0.03
26	1.535	0.058	1.538	0.25	0.21
27	1.662	0.21	1.681	0.28	1.16
28	1.644	0.175	1.654	0.21	0.60
29	1.597	0.1	1.877	0.39	17.52
30	1.536	0.045	1.752	0.27	14.07
		Average difference (%)			11.14

Discussion

The present work describes a methodology for manufacturing patient-specific replicas of arteries with regionally varying wall thickness, with a particular focus on developing AAA phantoms with patient-specific wall thickness distributions. The thickness

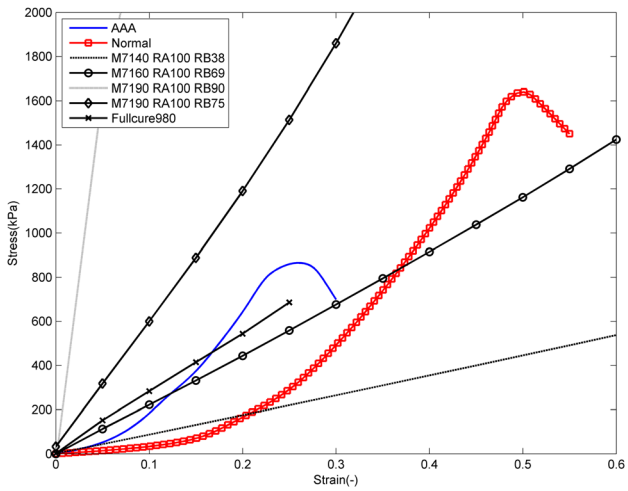

Fig. 5 Stress-strain curves for PUR resins and 3D printing versus ex vivo experiments for normal and AAA arteries from Raghavan and Vorp [11]

differences obtained from the comparison of the virtual and physical arteries are due to two main sources. On the one hand, the process for measuring the wall thickness in the physical artery was the most suitable to the model and is one that was followed similarly by Doyle and colleagues [7].

The methodology is not devoid of measuring errors. Depending on the user's skill, the material of the phantom could be more or less compressed when measuring the thickness. This limitation was evaluated with the help of 5 subjects who were asked to measure 10 times the thickness of a rectangular sample of the 7140 material with a uniform thickness of 2.5 mm. The fifth subject also measured the thickness values of the artery replica for this manuscript. An analysis of variance analysis was performed and showed that there are no statistically significant differences between the mean values for the thickness (p value $= 0.586$) meaning that inter-operator variability of the wall thickness measurements is not critical. With this in mind, our results showed that the error introduced by the fifth subject is 1.64%. It seems reasonable for the authors to expect a similar error when measuring the wall thickness of the artery replica.

On the other hand, it seems that the greater wall thickness of the phantom was due to the expansion of the silicone and the contraction of the wax. Wax contraction was mitigated by preheating the silicone mold and the AM artery inside it to 45 °C. The expansion of the silicone was difficult to minimize because each time the mold was used it exhibited some expansion. In vacuum casting, the silicone mold is normally discarded after 15–20 trials because of geometric and dimensional tolerance differences. The phantom we measured was obtained at the 3rd trial, such that the molds had undergone the casting process twice and thus had reasonable accuracy, as Table 1 illustrates.

The cost of manufacturing the artery replicas is relatively low when one considers that the main investment is the 3D printer, which is priced at approximately 100,000 €(∼132,420 USD). Although 3D printing technology is becoming more widespread, with 3D desktop printers currently priced as low as 300 USD, the cost of the technology at high resolutions still remains extraordinary for academic use. However, once the artery is printed and the silicone mold is made, the cost of a new replica is only 15 €(∼20 USD). Nevertheless, a limitation of the methodology is that after approximately 5–10 casting processes, a new silicone mold should be created to avoid possible dimensional inaccuracies in the resulting replica. Yet, in this worst case scenario in which it would be necessary to build both the artery with PUR resins and a new silicone mold in every casting, the cost would only increase to 55 €(∼72 USD).

Regarding the rubberlike materials available for the 3D printing, the response of the Fullcure 980 seems to be in range with the AAA and AA material properties arteries; in addition, it presents a better dimensional accuracy in the artery with respect to the methodology presented in this paper. However, an artery made of Fullcure 980 has three main disadvantages, which are not observed with the PUR approach. First, its stiffness is fixed, i.e., the user cannot control it and, consequently, the material cannot mimic the response of different patient-specific AAA properties. With the methodology used in this study we can achieve any individual stiffness by changing the mixing ratio of the PUR resins. Second, due to the printing with Fullcure 980, the artery has anisotropy in the three printing directions, which cannot be controlled. Finally, the cost of printing with Fullcure 980 is higher: for more than one AAA model, the AM process would cost 80 USD per replica since the artery needs to be printed every time.

The current tests and methodology were carried out at a room temperature of 20 °C and future experimental tests should be performed at that temperature. If the phantom needs to be analyzed at body temperature (37 °C), the protocol is still also valid, but the tensile tests should be repeated at 37 °C in order to take into account the new softer behavior of the PUR resins and to select the most appropriate PUR resin.

The methodology described herein was focused on building realistic AAA replicas with isotropic mechanical properties. Having control of the wall thickness and the stress-strain curve on an individual basis is a step forward in achieving the exact mechanical behavior of the vessel. The ongoing work is focused on addressing arterial anisotropic behavior by the addition of fibers of a second PUR resin during the manufacturing process.

Conclusion

This work represents the development and application of a novel methodology for building AAA replicas with patient-specific regionally varying nonuniform wall thickness and isotropic material properties at small strains. The method is fast, relatively inexpensive, and can be easily reproduced for other applications. Liquid polyurethane resins have shown to be appropriate materials to characterize the mechanical behavior of healthy arteries and aneurysmal aortas, in both in vitro (with no prestretch) and in vivo conditions (with prestretch).

References

[1] Upchurch, G. R., and Schaub, T. A., 2006, "Abdominal Aortic Aneurysm," Am. Fam. Phys., **73**(7), pp. 1198–1204. Available at http://www.aafp.org/afp/2006/0401/p1198.html

[2] The United Kingdom Small Aneurysm Trial Participants, 2002, "Long-Term Outcomes of Immediate Repair Compared With Surveillance of Small Abdominal Aortic Aneurysm," N. Engl. J. Med., **346**(19), pp. 1445–1452.

[3] Fillinger, M. F., Marra, S. P., Raghavan, M. L., and Kennedy, F. E., 2003, "Prediction of Rupture Risk in Abdominal Aortic Aneurysm During Observation: Wall Stress Versus Diameter," J. Vasc. Surg., **37**, pp. 724–732.

[4] Doyle, B. J., Callahan, A., and McGloughlin, T. M., 2007, "A Comparison of Modelling Techniques for Computing Wall Stress in Abdominal Aortic Aneurysm," Biomed. Eng. Online, **6**, p. 38.

[5] Doyle, B. J., Callahan, A., Walsh, M. T., Grace, P. A., and McGloughlin, T. M., 2009, "A Finite Element Analysis Rupture Index (FEARI) as an Additional Tool for Abdominal Aortic Aneurysm Rupture," Vasc. Dis. Prev., **6**, p. 114–121.

[6] Van de Geest, J. P., Di Martino, E. E., Bohra, A., Makaroum, M.S., and Vorp, D. A., 2006, "A Biomechanics-Based Rupture Potential Index for Abdominal Aortic Aneurysm Risk Assessment,". Ann. N.Y. Acad. Sci., **1085**, p. 11–21.

[7] Doyle, B. J., Morris, L. G., Callahan, A., Kelly, P., Vorp, D. A., and Mc Gloughli, T.M., 2008, "3D Reconstruction and Manufacture of Real Abdominal Aortic Aneurysms: From CT Scan to Silicone Model," ASME J. Biomech. Eng., **130**(3), p. 034501.

[8] O'Brien, T., Morris, L. G., O'Donnell, M., Walsh, M. T., and Mc Gloughlin, T. M., 2005, "Injection-Moulded Models of Major and Minor Arteries: The Variability of Model Wall Thickness Owing to Casting Technique," Proc. Inst. Mech. Eng., Part H: J. Eng. Med., 219, pp. 381–386.

[9] Raghavan, M. L., Kratzberg, E. M., Castro de Tolosa, E. M., Hanaoka, M. M., Walker, P., and Da Silva, E. S., 2006, "Regional Distribution of Wall Thickness and Failure Properties of Human Abdominal Aortic Aneurysm," J. Biomech., **39**(16), pp. 3010–3016.

[10] Doyle, B. J., Corbett, T. J., Cloonan, A. J., O'Donnell, M., Walsh, M. T., Vorp, D. A., and Mc Gloughli, T. M., 2009, "Experimental Modelling of Aortic Aneurysms: Novel Applications of Silicone Rubbers," Med. Eng. Phys., **31**, pp. 1002–1012.
[11] Raghavan, M. L., Webster, M. W., and Vorp, D. A., 1996, "Ex Vivo Biomechanical Behaviour of Abdominal Aortic Aneurysm: Assessment Using a New Mathematical Model," Ann. Biomed. Eng., **24**(5), pp. 573–582.
[12] Shum, J., DiMartino, E. S., Goldhamme, A., Goldman, D. H., Acker, L. C., Patel, G., Ng, J. H., Martufi, G., and Finol, E. A., 2010, "Semiautomatic Vessel Wall Detection and Quantification of Wall Thickness in Computed Tomography Images of Human Abdominal Aortic Aneurysms," Med. Phys., **37**(2), pp. 638–648.
[13] Martufi, G., Di Martino, E. S., Amon, C. H., Muluk, S. C., and Finol, E. A., 2009, "Three-Dimensional Geometrical Characterization of Abdominal Aortic Aneurysms: Image-Based Wall Thickness Distribution," ASME J. Biomech. Eng., **131**(6), p. 061015.
[14] Shum, J., Xu, A., Chatnuntawech, I., and Finol, E. A., 2011, "A Framework for the Automatic Generation of Surface Topologies for Abdominal Aortic Aneurysm Models," Ann. Biomech. Eng. **39**(1), pp. 249–259.
[15] Shum, J., Martufi, G., Di Martino, E., Washington, C. B., Grisafi, J., Muluk, S. C., and Finol, E. A., 2011, "Quantitative Assessment of Abdominal Aortic Aneurysm Geometry," Ann. Biomed. Eng., **39**(1), pp. 277–286.
[16] Lee, K., Zhu, J., Shum, J., Zhang, Y., Muluk, S. C., Chandra, A., Eskandari, M. K., and Finol, E. A., 2013, "Surface Curvature as a Classifier of Abdominal Aortic Aneurysms: A Comparative Analysis," Ann. Biomed. Eng., **31**(3), pp. 562–576.
[17] Raut, S., Jana, A., De Oliveira, V., Muluk, S. C., and Finol, E. A., 2013, "The Importance of Patient-Specific Regionally Varying Wall Thickness in Abdominal Aortic Aneurysm Biomechanics," ASME J. Biomech. Eng., **135**(8), p. 081010.
[18] Mullins, L., 1969, "Softening of Rubber by Deformation," Rubber Chem. Technol., **42**, pp. 339–362.
[19] Lu, J., Zhou, X., and Raghavan, M. L., 2007, "Inverse Elastostatic Stress Analysis in PreDeformed Biological Structures: Demonstration Using Abdominal Aortic Aneurysms," J. Biomech., **40**, pp. 693–696.
[20] Gee, M. W., Reeps, C., Eckstein, H. H., and Wall, W. A., 2009, "Prestressing in Finite Deformation Abdominal Aortic Aneurysm Simulation," J. Biomech., **42**, pp. 1732–1739.
[21] Speelman, L., Bosboom, E. M. H., Shurink, G. W. H., Buth, J., Breeuwer, M., Jacobs, M. J., and Van de Vosse, F. N., 2009, "Initial Stress and Nonlinear Material Behavior in Patient-Specific AAA Wall Stress Analysis," J. Biomech., **42**, pp. 1713–1719.
[22] Riveros, F., Chandra, S. C., Finol, E. A., Gasser, T. C., and Rodriguez, J. F., 2013, "A Pull-Back Algorithm to Determine the Unloaded Vascular Geometry in Anisotropic Hyperelastic AAA Passive Mechanics," Ann. Biomed.Eng., **41**, pp. 694–708.